PAPER

NJC
www.rsc.org/njc

Synthesis, X-ray characterization and study of new ionic complexes of 2-pyridone, obtained by oxidation with I_2

Constantinos D. Antoniadis,[a] Sotiris K. Hadjikakou,*[a] Nick Hadjiliadis,*[a] Maciej Kubicki[b] and Ian S. Butler[c]

[a] *Section of Inorganic and Analytical Chemistry, Department of Chemistry, University of Ioannina, 45110 Ioannina, Greece. E-mail: shadjika@cc.uoi.gr, nhadjis@cc.uoi.gr; Fax: +30-26510-44831; Tel: +30-26510-98374, +30-26510-98420*
[b] *Department of Chemistry, A. Mickiewicz University, ul. Grunwaldzka 6, 60-780 Poznan, Poland*
[c] *Department of Chemistry, McGill University, 801 Sherbrooke, Montreal, PQ, Canada H2A 2K6*

Received (in Montpellier, France) 19th November 2004, Accepted 19th January 2005
First published as an Advance Article on the web 30th March 2005

The reaction of 2-pyridone (C_5H_5NO or PYOH) with diiodine in molar ratios of 2 : 1 and 1 : 2 resulted in the formation of complexes $\{[(PYOH)_3(PYOH)^+]\cdot I_3^-\}$ (**1**) and $\{\{(PYOH)_6\cdot[(PYOH)_2]^{2+}\}\cdot 0.5I^-\cdot 1.5I_7^-\cdot I_2\}$ (**2**), respectively. The reactions were carried out in dichloromethane solutions in air. The compounds were characterized by elemental analysis, DTA-TGA chromatography, FT-Raman, FT-IR, UV-vis and EPR spectroscopies. Crystal structures of the named complexes have been determined by X-ray diffraction at 120(1) K (**1**) and 293(2) K (**2**). Compound **1**, $[(C_{20}H_{20}N_4O_4)I_3]$, monoclinic, space group $C2/c$, consists of a cationic $PYOH^+$ radical species and an I_3^- counter anion; three neutral PYOH molecules are also bound to the complex. The crystal structure of $[(C_{40}H_{40}N_8O_8)I_{13}]$ (**2**) reveals a centrosymmetric P-1 triclinic space group containing two cationic $PYOH^+$ species, with the anionic counterparts being one half I^- and three halves I_7^-. Also, a neutral diiodine molecule I_2 is retained by weak halogen-halogen interactions to I^-, as well as six neutral PYOH ligands. The structures of **1** and **2** consist of hydrogen-bonded pyridine layers; polyiodide fragments fill the spaces between the layers, additionally kept together by a number of weak C–H···I interactions.

Introduction

The perturbation of the I–I bond of diiodine by heterocycles such as thiones or selones is known to produce various types of compounds, including charge-transfer complexes, iodonium salts, "spoke structures", "extended spoke structures", monocationic disulfides and dicationic disulfides or diselenides.[1–2] On the other hand, the remarkable ability of iodine to catenate has led to the formation of an array of polyiodides offering a wide range of structures[3] that have been recently reviewed by Boyle and Godfrey, Deplano *et al.* and Svensson and Kloo.[4] The structural variety of polyiodides range from the simple I_3^- through the linear I_4^{2-}, V-shaped I_5^-, three-pronged structures of I_7^-, I_9^-, I_{10}^{2-}, and I_{12}^{2-}, Z-shaped I_7^- and I_8^{2-}, branched I_{16}^{2-}, and S-shaped and linear I_{16}^{4-} species to infinite chains.[3,4] The size and shape of polyiodide ions have been found to depend unpredictably on the size and shape of the counter ion. Also, in recent years, polyiodides have drawn considerable attention for their electrical properties.[5] Examples include superconductors, as in the case of the electrolytic oxidation of bis(ethylenedithio)tetrathiafulvalene (BEDT-TTF or ET) in the presence of triiodide anions, which leads to the ambient pressure organic superconductors β-$(ET)_2I_3$.[5a,b]

The perturbation of the I–I bond by pyridine and its derivatives, such as 2-pyridone (PYOH), can lead to other novel complexes containing polyiodides. The formation of these new complexes can be achieved by oxidation of 2-pyridone derivatives by diiodine. We intend to use PYOH to exploit the higher electronegativity of oxygen compared to sulfur or selenium in order to more strongly perturb the I–I bond and compare the resulting compounds with those described in the literature. Here, the synthesis and characterization of two new complexes of 2-pyridone, $\{[(PYOH)_3(PYOH)^+]\cdot I_3^-\}$ (**1**) and $\{\{(PYOH)_6\cdot[(PYOH)_2]^{2+}\}\cdot 0.5I^-\cdot 1.5I_7^-\cdot I_2\}$ (**2**), obtained by oxidation with I_2, are discussed.

DOI: 10.1039/b417828a

Results and discussion

Synthesis

The reaction between 2-pyridone (PYOH) and I_2 leads to the formation of complexes **1** or **2** , depending on the stoichiometry of diiodine used (Scheme 1). PYOH is oxidized to its corresponding cationic radical as evidenced by EPR spectroscopy (see below). This radical is found to be stabilized by strong hydrogen bonds, in contrast to that of 2-mercaptopyridine (PYSH), which was described to react with I_2 in a molar ratio of 1 : 2, oxidizing the ligand to a monocationic disulfide with the simultaneous formation of I_3^-.[1d]

Thermal decomposition

TGA/TDA thermal analysis in flowing nitrogen showed that complex **1** decomposes in two stages: the first stage (61–138 °C) is endothermic and involves a 10% mass loss, corresponding to evolution of the co-crystallized neutral molecule of PYOH (calcd. mass loss 12%) which has a lower m.p. than I_2; the second stage (140–232 °C) is also endothermic and involves a 88% mass loss associated to the loss of $\{[(PYOH)_2(PYOH)^+]\cdot I_3^-\}$ (calcd. 88%). I_3^- does not decompose and this indicates

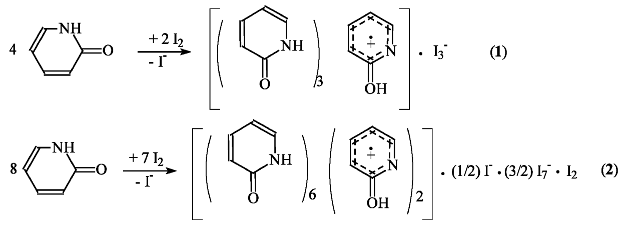

Scheme 1

that it has a symmetric structure in complex **1**[4b] (see also Raman data and crystal structure).

The corresponding thermal analysis of **2** shows a three-step decomposition. All stages are endothermic. The first stage (60–85 °C) involves a 12% mass loss, which is consistent with the evolution of three neutral molecules of PYOH (calcd. 12%). The second stage (85–115 °C) involves a 33% mass loss corresponding to the loss of three molecules of I_2 (calcd. 32%). Since there is only one I_2 molecule in **2**, the other two may derive from the decomposition of I_7^-, which may exist in the $I_2I_3^-I_2$ form[4b] (see crystal structure). The third step (117–196 °C) involves a loss of 56%, attributed to decomposition of the rest of the compound, that is, $\{(PYOH)_3 \cdot [(PYOH)_2]^{2+}\} \cdot 0.5I^- \cdot 1.5I_3^- \cdot I_2\}$ (calcd. 56%).

Conductivity measurements

Conductivity titration of PYOH with I_2 in acetonitrile is shown in Fig. 1. At $[I_2] = 0$, the system shows a low conductivity, because of the deprotonation equilibrium established in the solution (PYOH: $pK_a = 11.62$[6]). Then conductivity increases up to a $[I_2]:[PYOH]$ ratio of 1 : 2 (corresponding to the stoichiometry where complex **1** is formed, Scheme 1, eqn. 1), where it reaches a first plateau. A higher plateau is reached when the $[I_2]/[PYOH]$ ratio approaches 1, which corresponds almost to the stoichiometry of complex **2** (Scheme 1, eqn. 2). At ratios $[I_2]/[PYOH] > 2$ the conductivity reaches a third plateau and this may correspond to another complex with PYOH that has not been isolated.

Spectroscopic analysis

(A) EPR. The electron paramagnetic resonance spectrum of compound **2** contains a narrow $\Delta H = 6$ G, $g \sim 2$ signal, which can be assigned to an $S = 1/2$ organic radical. At room temperature, this signal saturates at 12 mW, which indicates that the radical is in close proximity with other paramagnetic spins. These spins might be adjacent radicals or, alternatively, other paramagnetic species, that is, the iodine-based paramagnetic clusters that exist in sample **2**. From control experiments we observed that such iodine-based clusters give EPR signals consisting of a strong triplet split by *ca.* 50 G.

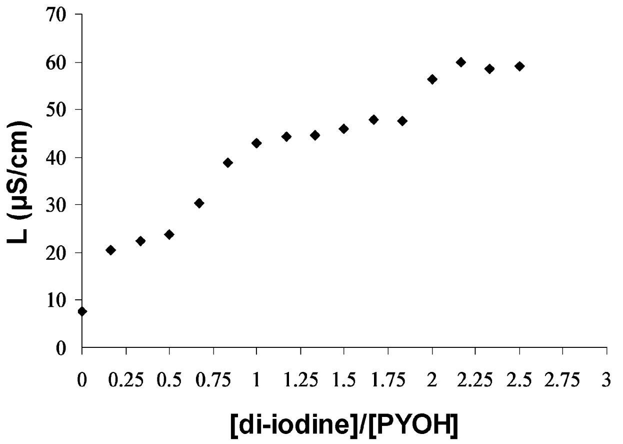

Fig. 1 Conductivity titration of 10^{-2} M PYOH with I_2 in acetonitrile ($T = 293$ K).

(B) UV-Vis. The UV-vis spectra of diiodine complexes **1** or **2** with 2-pyridone in dichloromethane are given in Fig. 2(A). **1** and **2** exhibit one distinct absorption band at 495–505 nm, which is assigned to the blue-shifted band of I_2,[1,2] occurring at 504 nm in free I_2 in CH_2Cl_2.[2e,g] The absorption band at 366 nm in **1** is assigned to the I_3^- species (λmax = 360 nm in free I_3^-).[7] The band at 362 nm in the spectrum of **2** may also be attributed to the I_3^- species, indicating a $I_2–I_3^-–I_2$ [4b] configuration for I_7^-, as previously suggested (see also crystal structure and Raman spectroscopy results). I_3^- has one more absorption band, observed at 297 nm in **1** and 294.5 nm in **2**. These, however, coincide with the intra-ligand transitions ($\pi^* \leftarrow \pi$) appearing at 302 nm in PYOH and they are very intense. Fig. 2(B) shows UV-vis spectra of dichloromethane solutions at a given PYOH concentration (10^{-4} M) and increasing quantities of diiodine. In these spectra, no isosbestic points are observed, indicating that more than two species are present in solution. Unexpectedly, no band was observed at 360–370 nm in the spectrophotometric titration curves of I_2–PYOH at any molar ratio, indicating that no I_3^- ions were formed in solution.

(C) Vibrational (IR and Raman). The IR spectra of complexes **1** and **2** show vibrational bands at 1618, 1155 and 570 cm^{-1}, which are attributed to the vibrations of the amide bonds. The new band appearing at 158 cm^{-1} in the far-IR spectrum of complexes **1** and **2** has been assigned to the ν(I–I) stretching vibration modes.[1a,8] Diiodine vapor exhibits a

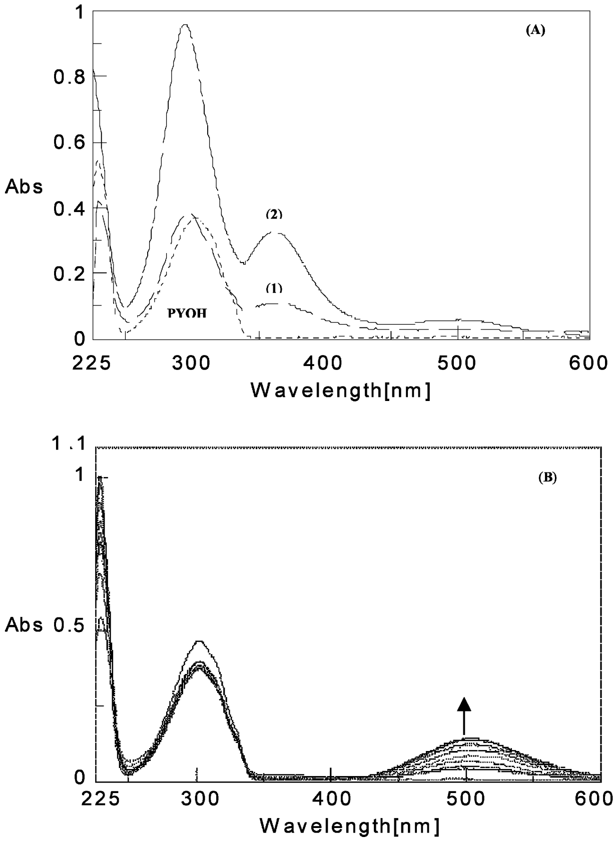

Fig. 2 (A) UV-Vis spectra of **1** (5×10^{-5} M, long dashed line), **2** (8.6×10^{-5} M, solid line) and PYOH (5×10^{-5} M, short dashed line) in dichloromethane. (B) UV-Vis spectra in dichloromethane with a fixed PYOH concentration (10^{-4} M) and increasing quantities of diiodine: $[I_2]/[L] = 0.33$ (1); 0.50 (2); 0.66 (3); 0.84 (4); 1.00 (5); 1.16 (6); 1.34 (7); 1.50 (8); 1.66 (9).

Table 1 Structural and Raman spectral data of complexes **1-2**

Compound	Iodine containing counter part	Geometry	d(I–I)/Å	Bond order n	Raman data/cm^{-1}
$\{[(PYOH)_3(PYOH)^+]\cdot I_3^-\}$ (**1**)	I_3^-: I–I–I	Linear symmetric	2.9131(5)	0.52	161.5 w, 108.0 s
$\{\{(PYOH)_6[(PYOH)_2]^{2+}\}\cdot 0.5I^-\cdot 1.5I_7^-\cdot I_2\}$ (**2**)	I^-	Zig-zag chains	2.946(2), 2.946(2), 3.173(2), 2.779(2)	0.47, 0.47, 0.26, 0.74	166.3 vs, 131.5 m, 108.4 s
	I_7^-: $I_2\cdot I_3^-\cdot I_2$		2.793(3), 3.328(3), 2.909(2), 2.933(2), 3.307(2), 2.759(2)	0.72, 0.17, 0.52, 0.49, 0.18, 0.79	

strong band at 216 cm^{-1} [ν(I–I)], which appears at 180 cm^{-1} in the solid state.[9] This shifts to lower wavenumbers upon coordination to a donor atom, reflecting the reduction in the I–I bond order as well as the strengthening of the complex formed.[1,2b,c,4b,10]

Table 1 gives structural and Raman spectral data in the region 300–50 cm^{-1} for complexes **1** and **2**. The Raman spectrum of complex **1** exhibits two bands at 161.5 (weak) and 108.0 (strong) cm^{-1}. Bands around 110 cm^{-1} are normally attributed to the ν_1 symmetric stretching of I_3^-, which, as a symmetric ion, exhibits only one Raman active band.[1a,b,4b] It is worth noting that, when a distortion of I_3^- occurs, additional bands at higher frequencies (140–130 cm^{-1}), corresponding to Raman active antisymmetric stretching, and lower frequencies (80–70 cm^{-1}), corresponding to deformation motions of asymmetric I_3^-, can be observed.[4b,11] Thus, here complex **1** is more likely to contain a symmetric I_3^- moiety (I–I–I covalent adduct). The Raman spectrum of complex **2** with bands at 166.3 (vs), 131.5 (m) and 108.4 (s) cm^{-1} (Table 1) is a typical spectrum of a heptaiodide, where the polyiodide chain has a zig-zag conformation described as an I_2–I_3^-–I_2 sequence,[4b] confirming previous observations (see also crystal structure).

Crystal and molecular structures

Structures containing polyiodide anions with cationic aromatic sandwich complexes as counterparts are very rare in the literature.[12] Selected crystal data for **1** and **2** are listed in Table 2 and their ORTEP diagrams are shown in Figs. 3 and 4, respectively.†

The crystal structure of compound **1** was solved and successfully refined in the centrosymmetric space group *C*2/*c*, with two crystallographically independent C_5H_5NO fragments in the asymmetric part of the unit cell. The analysis of the hydrogen bonding scheme shows, however, that there is some disorder in the structure: there is a short intermolecular O···O contact of 2.448 Å between molecules (A) related by a center of inversion (Fig. 3). This may be regarded as an indication that the real symmetry of the crystal is lower (noncentrosymmetric *Cc* space group) and that there are four different C_5H_5NO fragments, three of them being neutral, in the pyridone form, while the fourth is charged ($C_5H_6NO^+$, *cf.* Scheme 1). Due to the nature of the X-ray experiments (which are time- and space-averaging) the centro/noncentro ambiguity is unresolvable on the basis of the X-ray data alone (see, for example, ref. 13 and references therein). Attempts to refine this structure in the *Cc* space group were unsatisfactory due to the huge correlations between the parameters, related here by a pseudo center of symmetry. In this case, the deviation from the centrosymmetric arrangement involves only the position of one hydrogen atom. We have therefore decided to describe the structure in the centrosymmetric space group, with one hydroxyl hydrogen partially occupied (with s.o.f. 0.5). The three-dimensional structure consists of hydrogen-bonded double layers of pyridine fragments, while the I_3^- counter anions are located between the layers (Fig. 5) and weakly bound to the aromatic rings (*via* C–H···I interactions).

In the structure of **2** we met a similar problem of centro/noncentro ambiguity (two symmetry-independent short O···O distances of 2.437 and 2.448 Å); the structure is described in the centrosymmetric *P*-1 triclinic space group, with 6 neutral pyridone molecules and two cationic $C_5H_6NO^+$ species (*cf.* Scheme 1), but the symmetry may also be described as *P*1 with 12 neutral pyridone molecules and four cationic $C_5H_6NO^+$ species. In the unit cell of **2** there are therefore two asymmetric units with a total of four cationic radical PYOH$^+$ species and one I^- plus three I_7^- anionic counterparts. Also, two neutral diiodine molecules are retained by weak halogen-halogen interactions with an I^- anion and twelve neutral PYOH ligands. Each asymmetric unit of **2** contains two cationic PYOH$^+$ species and two anionic (0.5 I^- and 1.5 I_7^-) counterparts. A neutral I_2 molecule is retained by weak halogen-halogen interactions with I^- and by six neutral PYOH ligands. An extended network of intermolecular N–H···O and O–H···O hydrogen bonds is also observed in **2**; the structure consists of hydrogen-bonded pyridine/pyridinium layers (similar to **1**) and polyiodide fragments that fill up the spaces between the layers, which are connected to the layers by a number of weak C–H···I interactions (Fig. 6).

Selected bond lengths and angles for **1** and **2** are given in Tables 3 and 4. The C–O bond lengths found in **1** are 1.279(6) Å for the nonprotonated neutral pyridone rings and 1.282(6) Å for the protonated oxidized ring (Fig. 3). The corresponding bond distances in **2** vary from 1.30(2) to 1.32(2) Å for the protonated oxidized pyridone rings and 1.21(2) to 1.29(2) Å for the

Table 2 Crystal data and the structure refinement details for complexes **1** and **2**

	1	**2**
Empirical formula	$C_{20}H_{20}N_4O_4I_3$	$C_{40}H_{40}N_8O_8I_{13}$
FW	761.076	2918.102
T/K	120(1)	293(2)
Crystal system	Monoclinic	Triclinic
Space group	*C*2/*c*	*P*-1
a/Å	14.0652(11)	11.2119(16)
b/Å	15.6176(14)	12.6039(18)
c/Å	11.5015(11)	23.715(3)
α/°	90	78.545(12)
β/°	99.635(7)	76.688(12)
γ/°	90	86.422(12)
U/ Å^3	2490.8(4)	3195.3(8)
Z	4	2
ρ_{calcd}/g cm^{-3}	2.032	2.507
μ/mm^{-1}	3.797	6.346
Reflections collected	8005	21756
Independent reflections	3130	7622
R_{int}	0.070	0.099
R^a [$I > 2\sigma(I)$]	0.0469	0.0678
$wR_2{}^b$ [$I > 2\sigma(I)$]	0.1063	0.1430

^{a} $R = \Sigma||F_o| - |F_c||/\Sigma|F_o|$. ^{b} $wR_2 = [\Sigma w(F_o^2 - F_c^2)^2/\Sigma\, w(F_o^2)^2]^{1/2}$.

---

† CCDC reference numbers 230098 (**1**) and 230099 (**2**). See http://www.rsc.org/suppdata/nj/b4/b417828a/ for crystallographic data in .cif or other electronic format.

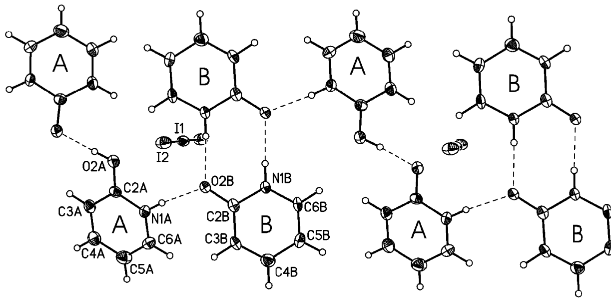

Fig. 3 ORTEP diagram of the ionic components of compound **1** together with the atomic numbering scheme. The displacement ellipsoids are drawn at the 50% probability level, hydrogen atoms are depicted as spheres of arbitrary radii. Relevant bond lengths are given in the text.

nonprotonated neutral pyridone rings (Fig. 4). Thus, the proton is located closer to the longer C–O bonds. Similarly, the corresponding C–O bond distances measured in {[(phenacetin)·(Hphenacetin)$^+$]·HI$_4^-$}[12a] [phenacetin = *N*-(4-ethoxyphenyl)acetamide] are 1.24(6) and 1.28(3) Å, respectively. The I–I bond distances in I$_3^-$ in complex **1** are equal to one another [2.9132(5) Å] due to the special position of the anion, on the center of symmetry; for the same reason the anion is perfectly linear (I–I–I bond angle 180.0°), in agreement with the Raman data. According to Pauling,[14a] $d(\text{I–I}) = d_o - 0.85\log(n)$, where d_o is the I–I bond distance for I$_2$ in the gas phase (2.67 Å [14b]) and n is the bond order. The calculated values of bond order for the I–I bonds of complexes **1** and **2** are listed in Table 1. Deplano *et al.* [4b] classified triiodide adducts into two types: (i) the I$^-\cdots$I$_2$ adducts, which have linear asymmetric geometry with one strong I–I bond (bond orders >0.63e) and one weaker I–I bond (bond orders <0.30e) and (ii) the covalent I–I–I complexes with either linear symmetric geometry (with two equivalent I–I bonds and bond order values around 0.50e) or linear asymmetric geometry (with two nonequivalent I–I bonds and bond order values also around 0.50e but with a stronger bond, bond order >0.50e, and a weaker one, bond order <0.50e). Thus, according to the observed values of I–I bond lengths and bond orders, complex **1** can be classified as containing symmetric I–I–I adducts.

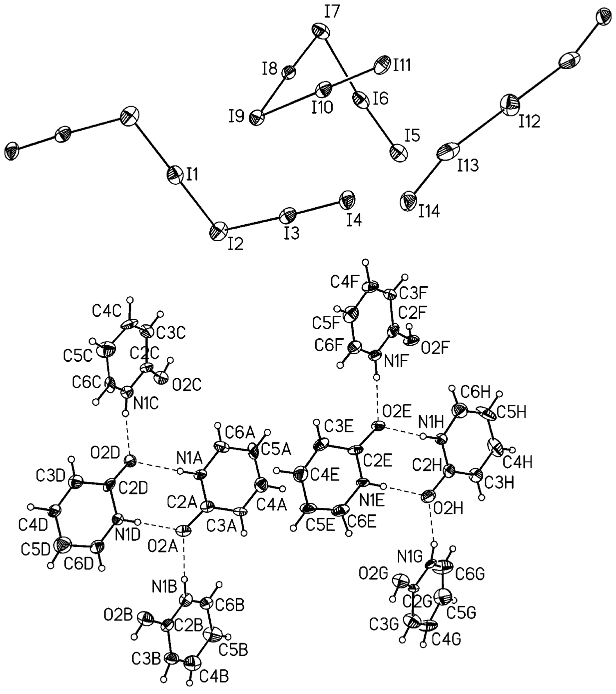

Fig. 4 ORTEP diagram of the ionic components of compound **2** together with the atomic numbering scheme. The displacement ellipsoids are drawn at the 50% probability level, hydrogen atoms are depicted as spheres of arbitrary radii. Relevant bond lengths are given in the text.

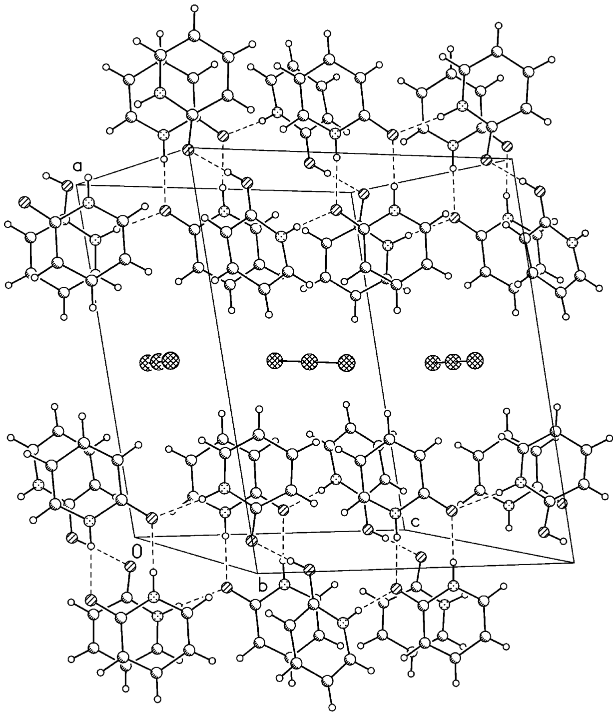

Fig. 5 Crystal packing of **1**. N–H···O and O–H···O hydrogen bonds are depicted as dashed lines.

Compound **2** contains two types of I$_7^-$ species, one symmetric and one asymmetric. The bond distances in symmetric I$_7^-$ species are: I(1)–I(2) = 2.946(2), I(2)–I(3) = 3.173(2) and I(3)–I(4) = 2.779(2) Å (Scheme 2). In asymmetric I$_7^-$ fragments, the bond distances are: I(5)–I(6) = 2.793(3), I(6)–I(7) = 3.328(3), I(7)–I(8) = 2.909(2), I(8)–I(9) = 2.933(2), I(9)–I(10) = 3.307(2) and I(10)–I(11) = 2.759(2) Å (Scheme 2). Deplano *et al.*[4b] classified heptaiodide adducts into two types. The first type includes heptaiodides described as a sequence of: I$_2$·I$_3^-$·I$_2$ with two short I–I bonds (in the range of the I–I bond in solid state diiodine, 2.715 Å [15]) with bond order values higher than 0.70e, two long I–I bonds distances with bond order values less than 0.20e and two I–I bonds that have intermediate lengths and bond order values around 0.50e. Heptaiodides of this type have a zig-zag geometry. In the second type, the heptaiodides show a pyramidal geometry and can be described as I$^-$·3I$_2$ adducts. In this type, heptaiodides have three short I–I bonds with bond order values higher than 0.70e and three long bond lengths with bond order values less than 0.30e. The

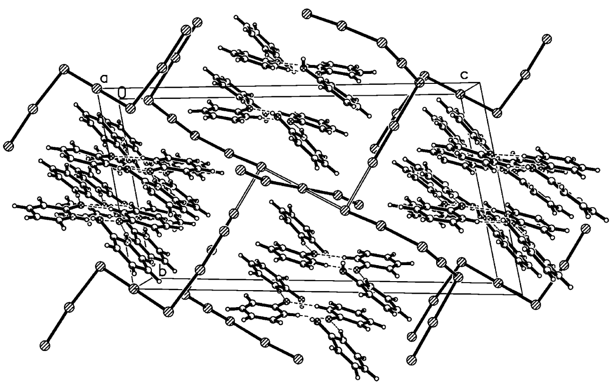

Fig. 6 Crystal packing of **2**. N–H···O and O–H···O hydrogen bonds are depicted as dashed lines; longer I···I interactions, creating the infinite polyanion of iodine species, are drawn as open lines.

Table 3 Selected bond lengths (Å) and angles (°) for compound **1**[a]

I(1)–I(2)	2.9131(5)	C(5A)–C(6A)	1.351(8)
I(1)–I(2)#1	2.9131(5)	C(2B)–O(2B)	1.282(6)
C(2A)–O(2A)	1.278(6)	N(1B)–C(6B)	1.371(7)
N(1A)–C(2A)	1.364(6)	N(1B)–C(2B)	1.369(7)
N(1A)–C(6A)	1.341(7)	C(2B)–C(3B)	1.408(8)
C(2A)–C(3A)	1.419(7)	C(3B)–C(4B)	1.361(8)
C(3A)–C(4A)	1.360(8)	C(4B)–C(5B)	1.407(8)
C(4A)–C(5A)	1.396(8)	C(5B)–C(6B)	1.347(8)
I(2)–I(1)–I(2)#1	180.0	C(2B)–N(1B)–C(6B)	122.5(5)
C(6A)–N(1A)–C(2A)	123.6(5)	O(2B)–C(2B)–N(1B)	117.3(5)
O(2A)–C(2A)–N(1A)	118.1(5)	O(2B)–C(2B)–C(3B)	126.1(5)
O(2A)–C(2A)–C(3A)	125.9(5)	N(1B)–C(2B)–C(3B)	116.6(5)
N(1A)–C(2A)–C(3A)	116.0(5)		

[a] Symmetry transformations used to generate equivalent atoms: #1 $-x+1$, $-y+1$, $-z+1$.

Table 4 Selected bond lengths (Å) and angles (°) for compound **2**[a]

I(1)–I(2)	2.946(2)	I(12)–I(13)	3.315(2)
I(1)–I(2)#1	2.946(2)	I(13)–I(14)	2.773(3)
I(2)–I(3)	3.173(2)	C(2A)–O(2A)	1.30(2)
I(3)–I(4)	2.779(2)	C(2B)–O(2B)	1.28(2)
I(5)–I(6)	2.793(2)	C(2C)–O(2C)	1.29(2)
I(6)–I(7)	3.328(3)	C(2D)–O(2D)	1.21(2)
I(7)–I(8)	2.909(2)	C(2E)–O(2E)	1.26(2)
I(8)–I(9)	2.933(2)	C(2F)–O(2F)	1.26(2)
I(9)–I(10)	3.307(2)	C(2G)–O(2G)	1.26(2)
I(10)–I(11)	2.759(2)	C(2H)–O(2H)	1.32(2)
I(2)–I(1)–I(2)#1	180.00(6)	I(7)–I(8)–I(9)	178.41(8)
I(1)–I(2)–I(3)	92.13(5)	I(8)–I(9)–I(10)	85.17(6)
I(4)–I(3)–I(2)	174.95(8)	I(11)–I(10)–I(9)	179.91(8)
I(5)–I(6)–I(7)	174.99(7)	I(14)–I(13)–I(12)	167.52(8)
I(8)–I(7)–I(6)	88.85(6)		

[a] Symmetry transformations used to generate equivalent atoms: #1 $-x$, $-y$, $-z$.

two long I–I bond distances measured in I_7^- species of **2**as well as their bond orders (Table 1) indicate that both I_7^- fragments are of the $I_2 \cdot I_3^- \cdot I_2$ type, in full agreement with Raman, thermal analysis and UV-vis observations.

The bond angles found in **2** follow the pattern found for other polyiodides[3–5]: The angles I(2)–I(1)–I(2)#1, I(2)–I(3)–I(4), I(5)–I(6)–I(7), I(7)–I(8)–I(9) and I(9)–I(10)–I(11) are close to 180° while the angles I(1)–I(2)–I(3), I(6)–I(7)–I(8) and I(8)–I(9)–I(10) are close to 90° (Fig. 4, Table 4). The torsion angles between three almost linear fragments of heptaiodides are different for two I_7^- anions: 180° for the I(1)···I(1A) fragment, but 92.2(1)° for I(5)···I(11). Two short I–I terminal bonds [I(13)–I(14), 2.774(3) Å], which are in the range of free diiodine (2.715 Å[15]) and two long central bonds [I(12)–I(13), 3.315(2) Å] indicate the retention of two neutral I_2 molecules in the unit cell of **2** with weak halogen-halogen interactions forming a weak centrosymmetric $I_2 \cdots I^- \cdots I_2$ complex. This anionic complex is almost linear (I–I–I angles along the anion are 180°, 167.5(1)° and 180°). Fig. 7 shows the polyiodide network established by weak halogen-halogen interactions, in the range 3.51–3.58 Å, between I_7^- and $I_2 \cdots I^- \cdots I_2$ ions. If only the I–I distances of 3.51 Å are taken into account, then an I_{19}^{3-} independent species may be considered (see Fig. 7), encompassing I(11) to I(11B) and including also I(14) to I(14A).

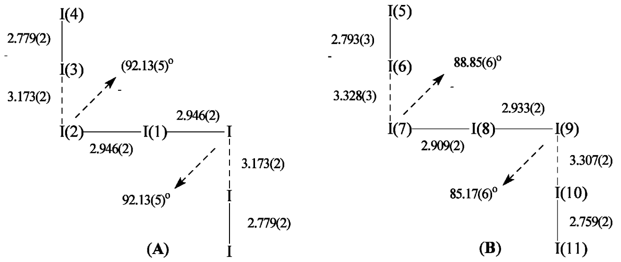

Scheme 2 Structural conformation of symmetric (A) and asymmetric (B) I_7^- ($I_2 \cdot I_3^- \cdot I_2$) moieties found in complex **2**.

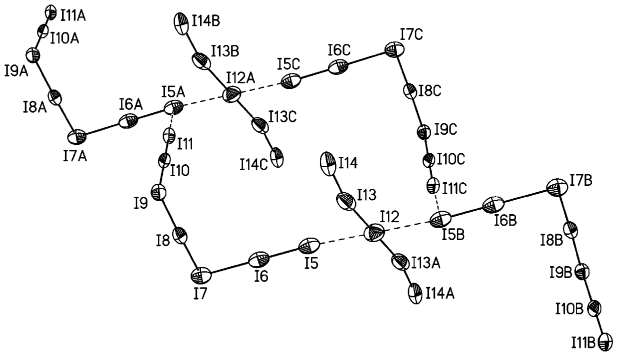

Fig. 7 Polyiodide network established by weak halogen-halogen interactions, in the distance range 3.51–3.58 Å, between I_7^- and $I_2 \cdots I^- \cdots I_2$ ions.

Conclusion

Structures containing polyiodide anions with cationic aromatic ligands as counterparts and having the general formula $\{[(L)(HL)^+] \cdot I_n^-\}$ are very rare in the literature and to the best of our knowledge there are only three other structurally characterized compounds of this type: $\{[(\text{phenacetin}) \cdot (\text{Hphenacetin})^+] \cdot HI_4^-\}$,[12a] $\{[(\text{phenacetin})(\text{Hphenacetin})^+] \cdot I_5^-\}$[12b] and $\{[(C_6H_5CONH_2)(C_6H_5CONH_3)^+] \cdot I_3^-\}$[12c] ($C_6H_5CONH_2$ = benzamide). The syntheses of these complexes were achieved by treatment of the appropriate amide with HI, in contrast to the present case of complexes **1** and **2**, formed by the direct reaction of 2-pyridone with diiodine in molar ratios of 2 : 1 and 1 : 2. This is a redox reaction[5a] where 2-pyridone is oxidized to a cationic radical. With 2-pyridone, however, peroxide structures are not formed, in contrast to the formation of disulfides in the case of PYSH.[1d] Here, polyiodide anions are simultaneously produced. This is probably a consequence of the redox differences between SH and OH groups and may prove to be a useful pathway for the synthesis of polyiodide materials.

Experimental

Materials and instruments

All solvents used were of reagent grade. Diiodine (Aldrich) and 2-pyridone (Merck) were used with no further purification.

Elemental analysis for C, H, N and S was carried out with a Carlo Erba EA model 1108 elemental analyzer. Melting points were measured in open tubes with a Stuart scientific apparatus and are uncorrected. Infrared spectra in the range 4000–370 cm^{-1} were obtained from KBr pellets, while far-IR spectra in the range 400–50 cm^{-1} were obtained from polyethylene pellets with a Perkin–Elmer Spectrum GX FT-IR spectrophotometer. A Jasco UV/Vis/NIR V 570 series spectrophotometer was used to record the electronic absorption spectra. Conductivity titrations were carried out at $T = 293$ K in acetonitrile solutions with a WTF LF-91 conductivity meter. Electron paramagnetic resonance spectra were recorded at room temperature on a Varian E-Line spectrometer operating at 9.26 GHz. Microwave power saturation experiments were performed by recording the signal intensity as a function of the microwave power in steps of 6 decibels.

Syntheses

Complexes **1** and **2** were prepared by mixing dichloromethane solutions of diiodine with dichloromethane solutions of 2-hydroxypyridine in the appropriate molar ratios, in air at 0 °C under continuous stirring for 4 h. The solutions were subsequently filtered and the resulting clear solutions were kept in the refrigerator for several days; crystals of the pure compounds formed and were filtered off. The filtrates were kept for further crystallization.

Complex 1. I_2: 0.127 g, 0.5 mmol; PYOH: 0.096 g, 1 mmol; CH_2Cl_2: 20 ml; m.p. 121–124 °C; anal. calcd for $C_{20}H_{20}N_4O_4I_3$: C: 31.56; H: 2.65, N: 7.36; found: C: 31.56; H: 0.63; N: 2.80; S: 14.07 %; IR (cm^{-1}): 3261 w, 1654 vs, 1611 s, 1541 s, 1436 s, 1240 m, 1150 m, 990 m, 770 vs, 722 s, 615 s, 569 s, 504 s, 157 m, 112 m; UV-vis [λ_{max}/nm (logε) in CH_2Cl_2]: 505 (2.77), 365 (3.44), 297 (3.89).

Complex 2. I_2: 0.254 g, 1 mmol; PYOH: 0.048 g, 0.5 mmol; CH_2Cl_2: 20 ml; m.p. 85–88 °C; anal. calcd for $C_{40}H_{40}N_8O_8)I_{13}$: C: 19.93; H: 1.67, N: 4.65; found: C: 19.65; H: 1.68; N: 4.77 %; IR (cm^{-1}): 3119 w, 1648 vs, 1617 s, 1540 s, 1430 s, 1250 m, 990 m, 771 vs, 720 s, 616 s, 570 s, 513 s, 151 vs; UV-vis [λ_{max}/nm (logε) in CH_2Cl_2]: 501.5 (2.83), 362 (3.58), 294.5 (4.05).

X-Ray structure determination

Dark crystals of the complexes suitable for single crystal analysis by X-ray crystallography were grown by slow evaporation of the filtrates from the reaction medium. Data were collected by the ω scan technique in the range $22.94° < 2\theta <$ to 29.35° for **1** and $2.70° < 2\theta <$ to 22.00° for **2** on a KUMA KM4CCD four-circle diffractometer[16a] with a CCD detector, using graphite-monochromated MoKα ($\lambda = 0.71073$ Å) at 120(1) K (**1**) and 293(2) (**2**). Cell parameters were determined by a least-squares fit.[16b] All data were corrected for Lorentz polarization effects and absorption.[16b,16c] The crystals of **2** were of relatively poor quality, therefore the statistical indicators of the appropriate refinements are not very good and the refinements were performed with constraints. Nevertheless, the quality of the data obtained allow for a reasonable discussion, especially on crystal packing and constitution of the complexes. The structures were solved with direct methods with SHELXS97[16d] and refined by full-matrix least-squares procedures on F^2 with SHELXL97.[16e] All nonhydrogen atoms were refined anisotropically; hydrogen atoms were located at calculated positions and refined as a riding model with isotropic thermal parameters fixed at 1.2 times the U_{eq} of the carrier atom.

In the structures of **1** and **2** some OH and NH hydrogen atoms were found to be disordered between the hydrogen-bonded molecules and were refined with site occupation factors of 1/2. This might be regarded as an indication that the symmetry of the space group should be lower. In this case, the structure would consist of antiparallel hydrogen-bonded chains made up of ordered molecules.

Acknowledgements

This work was carried out in partial fulfilment of the requirements for the M.Sc. thesis of Mr. C.D.A. within the graduate program EPEAEK in Bioinorganic Chemistry financed by the Ministry of Education of Greece and coordinated by Prof. N. Hadjiliadis. The NATO grant awarded to N.H. and I.S.B. is also acknowledged. We thank Dr. A. K. Zarkadis and Dr. I. Deligiannakis for helpful discussions on EPR spectra.

References

1 (*a*) V. Daga, S. K. Hadjikakou, N. Hadjiliadis, M. Kubicki, J. H. Z. dos Santos and I. S. Butler, *Eur. J. Inorg. Chem.*, 2002, 1718–1728; (*b*) J. H. Z. dos Santos, I. S. Butler, V. Daga, S. K. Hadjikakou and N. Hadjiliadis, *Spectrochim. Acta, Part A*, 2002, **58**, 2725–2735; (*c*) C. D. Antoniadis, G. Corban, S. K. Hadjikakou, N. Hadjiliadis, M. Kubicki, S. Warner and I. S. Butler, *Eur. J. Inorg. Chem.*, 2003, 1635–1640; (*d*) C. D. Antoniadis, S. K. Hadjikakou, N. Hadjiliadis, M. Kubicki and Ian S. Butler, *Eur. J. Inorg. Chem.*, 2004, 4324–4329; (*e*) G. J. Corban, S. K. Hadjikakou, N. Hadjiliadis, M. Kubicki, E. R. T. Tiekink, I. S. Butler, E. Drougas and A. M. Kosmas, submitted for publication.

2 (*a*) M. Esseffar, W. Bouab, A. Lamsabhi, J. L. M. Abboud, R. Notario and M. Yanez, *J. Am. Chem. Soc.*, 2000, **122**, 2300–2308; (*b*) F. Bigoli, P. Deplano, A. Ienco, C. Mealli, M. L. Mercuri, M. A. Pellinghelli, G. Pintus, G. Saba and E. F. Trogu, *Inorg. Chem.*, 1999, **38**, 4626–4636; (*c*) F. Bigoli, P. Deplano, M. L. Mercuri, M. A. Pellinghelli, A. Sabatini, E. F. Trogu and A. Vacca, *J. Chem. Soc., Dalton Trans.*, 1996, 3583–3598; (*d*) F. Freeman, J. W. Zi1ler, H. N. Po and M. C. Keindl, *J. Am. Chem. Soc.*, 1988, **110**, 2586–2591; (*e*) D. Arzei, P. Deplano, E. F. Trogu, F. Bigou, M. A. Pellinghelli and A. Vacca, *Can. J. Chem.*, 1988, **66**, 1483–1489; (*f*) F. Cristiani, F. A. Devillanova, A. Diaz and G. Verani, *J. Chem. Soc., Perkin Trans. 2*, 1984, 1383–1386; (*g*) F. A. Devillanova and G. Verani, *Tetrahedron*, 1979, **35**, 511–514; (*h*) M. C. Aragoni, M. Arca, F. Demartin, F. A. Devillanova, A. Garau, F. Isaia, V. Lippolis and G. O. Verani, *J. Am. Chem. Soc.*, 2002, **124**, 4538–4539.

3 (*a*) P. Coppens, in *Extended Linear Chain Compounds*, ed. J. S. Miller, Plenum Press, New York, 1982, p. 333; (*b*) G. A. Landrum, N. Goldberg and R. Hoffman, *J. Chem. Soc., Dalton Trans.*, 1997, 3605–3613; (*c*) S. Menon and M. V. Rajasekharan, *Inorg. Chem.*, 1997, **36**, 4983–4987; (*d*) K. F. Tebbe and S. Nafepour, *Acta Crystallogr., Sect. C*, 1994, **50**, 171–173; (*e*) F. H. Herbstein and W. Schwotzer, *Angew. Chem,. Int. Ed. Engl.*, 1982, **21**, 219–219; (*f*) P. C. Junk, L. R. McGillivray, M. T. May, K. D. Robinson and J. L. Atwood, *Inorg. Chem.*, 1995, **34**, 5395–5396; (*g*) P. K. Han, T. C. W. Mak and J. Trotter, *Inorg. Chem.*, 1979, **18**, 2916–2918; (*h*) D. B. Morse, T. B. Rauchfuss and S. R. Wilson, *J. Am. Chem. Soc.*, 1990, **112**, 1860–1864; (*i*) F. H. Herbstein and M. Kapon, *J. Chem. Soc., Chem. Commun.*, 1975, 677–678; (*j*) U. Behrens, H. J. Breunig, M. Denker and K. H. Ebert, *Angew. Chem., Int. Ed. Engl.*, 1994, **33**, 987–989; (*k*) K.-F. Tebbe and R. Buchem, *Angew. Chem., Int. Ed.*, 1997, **36**, 1345–1346.

4 (*a*) P. D. Boyle and S. M. Godfrey, *Coord. Chem. Rev.*, 2001, **223**, 265–299; (*b*) P. Deplano, J. R. Ferraro, M. L. Mercuri and E. F. Trogu, *Coord. Chem. Rev.*, 1999, **188**, 71–95; (*c*) P. H. Svensson and L. Kloo, *Chem. Rev.*, 2003, **103**, 1649–1684.

5 (*a*) M. A. Beno, U. Geiser, K. L. Kostka, H. H. Wang, K. S. Webb, M. A. Firestone, K. D. Cadson, L. Nuiiez, M.-H. Whangbo and J. M. Williams, *Inorg. Chem.*, 1987, **26**, 1912–1920; (*b*) J. M. Williams, T. J. Emge, H. H. Wang, M. A. Beno, P. T. Copps, L. N. Hall, K. D. Carlson and G. W. Crabtree, *Inorg. Chem.*, 1984, **23**, 2558–2560; (*c*) E. B. Yagubski, I. F. Shchegolev, V. N. Laukhin, P. A. Kononovich, M. V. Karatsovnik, A. V. Zvarykina and L. I. Buravov, *JETP Lett. Engl. Transl.*, 1984, **39**, 12–16; (*d*) T. Naito, A. Tateno, T. Udagawa, H. Kobayashi, R. Kato, A. Kobayashi and T. Nogami, *J. Chem. Soc., Faraday Trans.*, 1994, **90**, 763; (*e*) D. Davis, H. Gutfreund and W. A. Little, *Phys. Rev. B*, 1976, **13**, 4766; (*f*) B. A. Bolton and P. N. Prasad,

Mol. Cryst. Liq. Cryst., 1981, **76**, 309; (*g*) P. Coppens, P. C. W. Leung, R. Ortega, W. S. Young and C. Laporta, *J. Phys. Chem.*, 1983, **87**, 3355–3359.

6 C. Altomare, S. Cellamare, L. Summo, P. Fossa, L. Mosti and A. Carotti, *Bioorg. Med. Chem.*, 2000, **8**, 909–916.

7 (*a*) A. Suszuka, *J. Chem. Soc., Perkin Trans. 2*, 1985, 531–534; (*b*) A. I. Popov and N. E. Skelly, *J. Am. Chem. Soc.*, 1955, **77**, 3722–3724.

8 P. J. Hendra and N. Sadasivan, *Spectrochim. Acta*, 1965, **21**, 1127–1133.

9 (*a*) A. Anderson and T. S. Sun, *Chem. Phys. Lett.*, 1970, **6**, 611–616; (*b*) P. Deplano, F. A. Devillanova, J. R. Ferraro, F. Isaia, V. Lip-polis and M. L. Mercuri, *Appl. Spectrosc.*, 1992, **46**, 1625–1629.

10 F. Demartin, P. Deplano, F. A. Devillanova, F. Isaia, V. Lippolis and G. Verani, *Inorg. Chem.*, 1993, **32**, 3694–3699.

11 (*a*) P. D. Boyle, J. Christie, T. Dyer, S. M. Godfrey, I. R. Howson, C. McArthur, B. Omar, R. G. Pritchard and G. R. Williams, *J. Chem. Soc., Dalton Trans.*, 2000, 3106–3112; (*b*) F. H. Herbstein and W. Schwotzer, *J. Am. Chem. Soc.*, 1984, **106**, 2367–2373.

12 (*a*) F. H. Herbstein, M. Kapon and W. Schwotzer, *Helv. Chim. Acta*, 1983, **66**, 35–43; (*b*) F. H. Herbstein and M. Kapon, *Philos. Trans. R.. Soc. London, Ser. A*, 1979, **291**, 199–201; (*c*) J. M. Reddy, K. Knox and M. B. Robin, *J. Chem. Phys.*, 1964, **40**, 1082–1089.

13 M. Kubicki, T. Borowiak, G. Dutkiewicz, S. Sobiak and I. Weidlich, *Acta Crystallogr., Sect. B*, 2003, **59**, 487–491.

14 (*a*) L. Pauling, *The Nature of the Chemical Bond*, Cornell University Press, Ithaca, NY, 3rd edn., 1960; (*b*) H. B. Burgi, *Angew. Chem., Int. Ed. Eng.*, 1975, **14**, 460–473.

15 F. Van Bolhuis, P. B. Koster and T. Migchelsen, *Acta Crystallogr.*, 1967, **23**, 90–91.

16 (*a*) *KUMA KM-4CCD User Manual*, KUMA Diffraction, Wroclaw, Poland, 1999; (*b*) *CrysAlis, Program for Reduction of the Data from KUMA CCD Diffractometer*, KUMA Diffraction, Wroclaw, Poland, 1999; (*c*) R. H. Blessing, *J. Appl. Crystallogr.*, 1989, **22**, 396; (*d*) G. M. Sheldrick, *SHELXS-97, Program for solution of crystal structures*, University of Göttingen, Germany, 1997; (*e*) G. M. Sheldrick, *SHELXL-97, Program for refinement of crystal structures*, University of Göttingen, Germany, 1997.